

Polymer film-based optical access to enclosed gas: demonstration of H₂O absorption tomography

Ze Wang¹  · Mark H. Anderson² · Scott T. Sanders¹

Received: 7 July 2016 / Accepted: 18 August 2016 / Published online: 25 August 2016
© Springer-Verlag Berlin Heidelberg 2016

Abstract We demonstrate the use of a film to enable optical access to enclosed gases. We use absorption tomography to image H₂O in a 101.6-mm-diameter duct with 2-mm spatial resolution. Considering the central 94 mm, the standard deviation of the image is 1.6 %, and the average mole fraction error is −0.008 %. A polybenzimidazole film is identified to be a candidate for extending the technique to enable NH₃ imaging in a diesel aftertreatment system.

1 Introduction

Many researchers have demonstrated gas property imaging using absorption spectroscopy. Generally, the technique has either been applied to open flows allowing full optical access [1–7] or to enclosed flows with limited optical access [8, 9]. Here, we demonstrate the use of a film to allow full optical access to enclosed gases. We demonstrate the capability to measure 2-D distributions of H₂O mole fraction with a resolution of 2 mm.

Our motivation is tomography in a heavy-duty diesel aftertreatment system [9, 10]. Compared to our backscatter approach [10], tomography can work at any measurement plane with lower noise and higher throughput. Backscatter probes, on the other hand, use just one hole versus an entire wrap of film and require less equipment.

The films described in this paper have thicknesses of ~25 μm; this small dimension offers important advantages for optical access. First, the film exhibits significant transmission over a broad range of wavelengths. Second, it deflects laser beams negligibly by refraction. Third, the free spectral range of transmission etalons is ~100 cm⁻¹, large enough not to interfere with spectroscopy of most small molecules. Fourth, the film is pliable enough to conform to test article geometries; we wrapped the film around a pipe in this work.

2 Experimental setup

In our experiment, a distributed feedback (DFB) laser (NEL NLK1B5GAAA) operating near 1368.6 nm was used to monitor H₂O absorption. The laser targeted a H₂O feature that is strong at 25 °C and has favorable isolation from neighboring features. The linecenter and lower-state energy of the strongest transition in the target feature are 7306.7521 and 79.4964 cm⁻¹, respectively. The DFB laser was scanned over a spectral range of 5 cm⁻¹ at 5 kHz repetition rate. The scan waveform is provided by a function generator (Agilent 33250A).

The test article we studied is shown in Fig. 1. The gas flow of interest was enclosed within a stainless steel pipe with an outer diameter of 101.6 mm and a wall thickness of 1.7 mm. The pipe was cut at the location of the measurement plane. The two pipe sections remaining were oriented horizontally and coaxially, separated by 14.8 mm. A 30-mm-wide strip of film (Kapton HN, refractive index = 1.7), 0.02-mm thick, was wrapped around the 14.8-mm gap and sealed to both of the pipe sections using a tape (3 M Scotch 810). The two ends of the strip that met after being wrapped were also sealed to each other using

✉ Ze Wang
wangze925@gmail.com

¹ Mechanical Engineering Department, University of Wisconsin – Madison, 1500 Engineering Dr., Madison, WI 53706, USA

² Engineering Physics Department, University of Wisconsin – Madison, 1500 Engineering Dr., Madison, WI 53706, USA

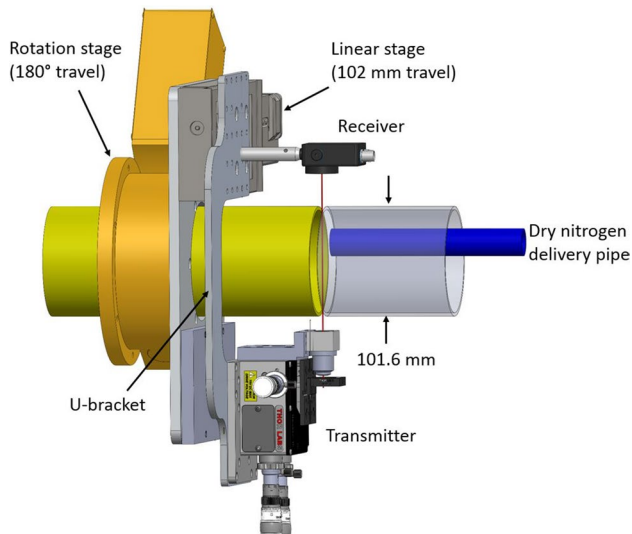


Fig. 1 Schematic of the test article. The blue tube supplied dry nitrogen in the nonuniform humidity test case. The entire setup shown was operated within an environmental chamber (Tesco WTH0208) maintained at $T = 298.15$ K, $X_{\text{H}_2\text{O}} = 0.0078$

a 1-mm-wide piece of the same tape. A single U-bracket was used to move the transmitter and receiver together. The laser beam was collimated by an aspheric lens (Newport 5723, 6.2-mm focal length). The transmitted beam was detected by a photodiode (Thorlabs PDA20CS-NOWIN-SP, 10 dB gain setting). The photodiode signal was logged by a digitizer (National Instruments PXI-5922).

A rotation stage (Newport RV160PP) was used to obtain data at each of 60 view angles. A linear stage (Newport UTS100PP) was used to obtain data at each of the 52 positions, for each angle.

Flexible ducts were connected to the remaining two pipe ends to manage the gas properties inside the test section. Using the ducts along with a ducted fan (Suncourt DB310P), air with known temperature and humidity was supplied to the test section from a second environmental chamber (Tesco WTH0208). Fans operating in each environmental chamber ensure uniform gas properties in our measurement plane. However, a second metal pipe (24-mm inner diameter, shown blue in Fig. 1) was optionally inserted through the flexible duct and positioned so it exhausted dry nitrogen at the measurement plane, creating a nonuniform H_2O mole fraction at the measurement plane. The measurement plane is approximately 1-mm downstream of the exit plane of the 24-mm pipe. The gas flow rates were set so that the distribution of gas velocity at the measurement plane remained approximately uniform at ~ 0.3 m/s.

The data collection process is as follows. The rotation stage and the linear stage each start at position 0. At this position, the data acquisition is triggered by the function

generator and subsequently records a 1000-point spectrum at 5 MS/s (a 200 μs record). Then, the linear stage is moved to the next linear location (a 2-mm increment), and the next spectrum is collected. Once spectra for all 52 linear locations have been recorded, the rotation stage is incremented by 3° . Data collection continues until all spectra have been collected (60 angles \times 52 positions = 3120 total spectra). The total data record length is 200 μs /spectrum \times 3120 spectra = 0.62 s, whereas the total time required to log the data is 30 min because of the time required for stage motion.

We used the signal removal method [11] to fit the baseline to the raw spectra and thereby obtain the absorption spectra. Then, we used a peak finding algorithm to find 3120 absorbance (α) values. When the beam strikes the tape that seals the two ends of the strip of film together, it scatters resulting in unusable signal level. Therefore, the absorbances for these locations (approximately, 40 out of 3120) were interpolated using the data from adjacent linear stage positions.

Because the environment surrounding the film had non-negligible humidity, a correction was required. We capped both ends of the pipe and purged the entire pipe with dry nitrogen. We measured all 3120 absorbance values for this purged case, and then subtracted each value accordingly. After this correction, only the humidity enclosed by the film was imaged. In a practical application, it may be impossible to purge the test article in this fashion. In that case, one can measure the ambient absorber concentration and then compute the correction based solely on geometry, as in [3].

3 Results

The 3120 absorbance values populate a 60×52 matrix (angles \times positions) of line integral data. The inverse radon routine in MATLAB was used to reduce this matrix to the absorbance image. We scaled the absorbance image to obtain the mole fraction, X , image using Eq. (1) from [10]:

$$k'_v * L * X = \alpha, \quad (1)$$

where L is the step size for the linear stage, 2 mm. For the feature we used near 1368.6 nm, $k'_v = 1.463 \text{ cm}^{-1}$ at $T = 298.15$ K, and $P = 0.969$ atm (0.982 bar). The resulting images are shown in Figs. 2 and 3. Considering only the central 94 mm of the uniform case, the standard deviation is 1.6 %, and the average mole fraction error (based on comparison with a thin film capacitance hygrometer) is -0.008 %. Considering the full reconstruction region of the uniform case, the standard deviation is 8.6 % and the average mole fraction error is -1.8 %. The error for the full image is higher, because the lower mole fractions along

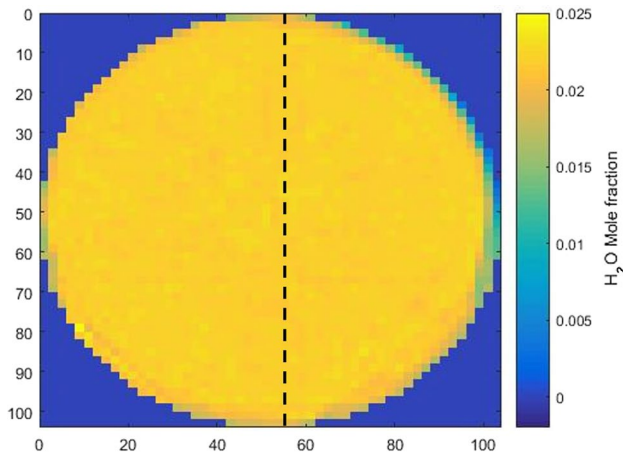


Fig. 2 Measured mole fraction image for the uniform case. The black line marks the line profile shown in Fig. 4

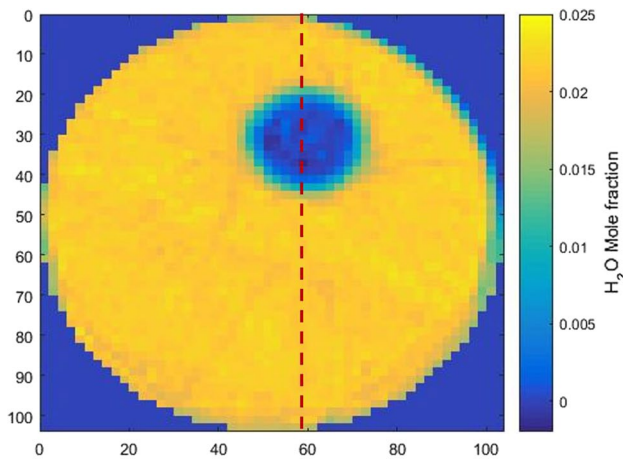


Fig. 3 Measured mole fraction image for the nonuniform case in which dry nitrogen was supplied to the test plane through a pipe with a 24-mm inner diameter. The red line marks the line profile shown in Fig. 4

the boundary are included. The linear stage travel was only 102 mm, and the center point of the stage assembly was not perfectly concentric with the 101.6-mm-diameter film enclosure. Accordingly, the entire boundary of the film is not captured on the image. Only the boundary shown in the top right of the images is captured correctly. In the other three quadrants of the image, the film boundary falls on or outside the reconstruction region; those boundaries appear sharper (Fig. 4).

4 Extension to other species

In diesel aftertreatment systems, other species such as NH₃ and NO are generally more important to measure than

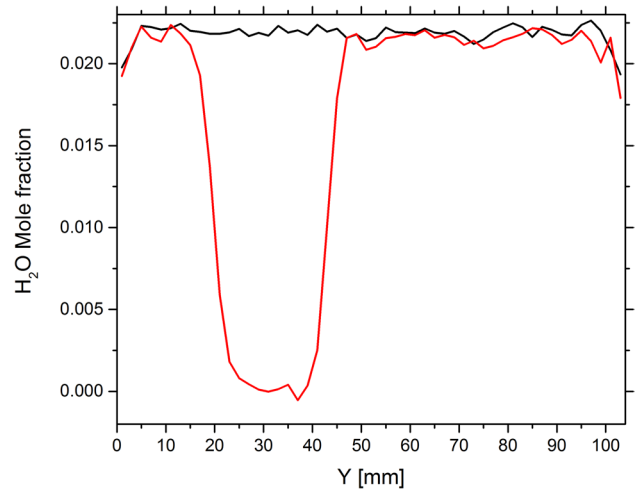


Fig. 4 Line profiles for the lines labeled in Figs. 2 and 3

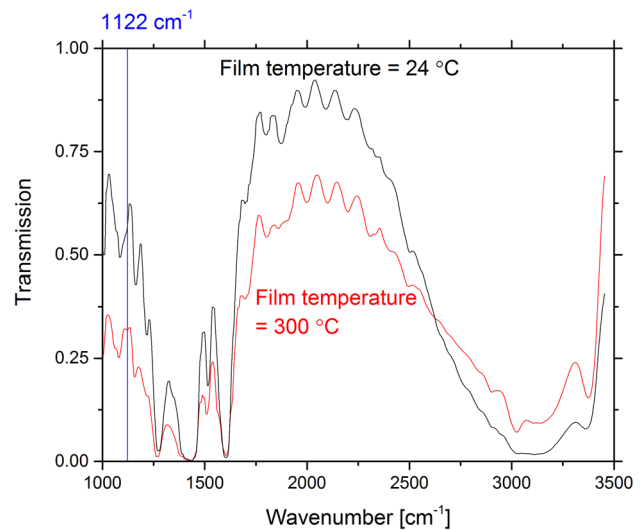


Fig. 5 FTIR results for FuMaTech PBI film (30- μ m thick) from 1000 to 3500 cm^{-1} . The blue vertical cursor at 1122 cm^{-1} (8.91 μm) marks the location of an attractive NH₃ absorption transition. The oscillations (visible, e.g., from 1750 to 2500 cm^{-1}) are due to an etalon formed by the parallel surfaces of the film

H₂O. Of the other important species, NH₃ presents a particular measurement challenge in the sense that a favorable measurement wavelength is near 8.91 μm . Most window materials have poor transmission at this wavelength, whether at room temperature (e.g., SiO₂, Al₂O₃) or at typical aftertreatment system external temperatures like 300 °C (e.g., Si, Ge). Other materials (e.g., BaF₂, CaF₂, ZnSe) can degrade when exposed to combustion product gases at such temperatures. Fortunately, polybenzimidazole (PBI) film (FuMaTech FUMAPEM[®] AP-30, refractive index = 1.696) is an attractive candidate and can be used in the same way

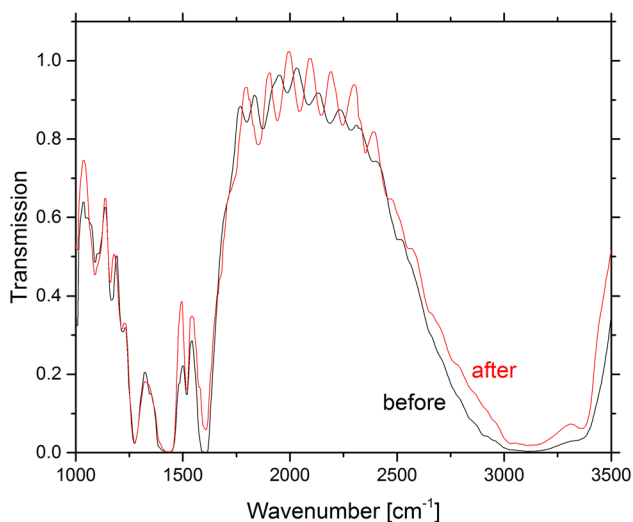


Fig. 6 FTIR results for FuMaTech PBI film at room temperature. A black trace is recorded before baking the film for 3 h at 300 °C. A red trace is recorded after cooling back to room temperature

as we used the film in the present work. We measured the transmission of this film (30 μm thick) using an FTIR spectrometer; the results are shown in Fig. 5. The transmission at 8.91 μm (1122 cm^{-1}) and 300 °C (after 1 h) is 32 %, sufficient for absorption tomography. An NH_3 transition near 10.39 μm (962.5 cm^{-1}) has also been used recently [12] and is likely to be accessible using a PBI film. Furthermore, the film is expected to maintain reliable mechanical properties up to at least 300 °C: a similar film (PBI Performance Products Celazole PBI) has a tear strength of 257 and 154 kN/m at 23 and 300 °C, respectively. The glass transition temperature for Celazole PBI film is 700 K, so in systems with external temperatures near 700 K the film is not likely to perform well. In another test of endurance of high temperature, we baked the FuMaTech PBI film for 3 h. The transmission measured before and after the high-temperature exposure are shown in Fig. 6.

5 Conclusions

We have demonstrated the use of a film to provide optical access in tomography. A PBI film is identified as valuable for NH_3 measurements. In the future, film optical access tomography could be operated at higher rates, for example using many emitters and detectors as demonstrated for liquid flows in pipes [13] or using cameras [14].

Acknowledgments The authors thank Mike Robinson of Cummins, Inc. for providing measurement hardware such as the stainless duct and Michael Zupan of Mark Anderson's lab for assistance in the FTIR work.

References

1. X. An, T. Kraetschmer, K. Takami, S.T. Sanders, L. Ma, W. Cai, X. Li, S. Roy, J.R. Gord, *Appl. Opt.* **50**, A29 (2011)
2. L. Ma, X. Li, S.T. Sanders, A.W. Caswell, S. Roy, D.H. Plemmons, J.R. Gord, *Opt. Express* **21**, 1152 (2013)
3. X. An, M.S. Brittelle, P.T. Lauzier, J.R. Gord, S. Roy, G.-H. Chen, S.T. Sanders, *Appl. Opt.* **54**, 9190 (2015)
4. L. Ma, W. Cai, A.W. Caswell, T. Kraetschmer, S.T. Sanders, S. Roy, J.R. Gord, *Opt. Express* **17**, 8602 (2009)
5. J.A. Silver, D.J. Kane, P.S. Greenberg, *Appl. Opt.* **34**, 2787 (1995)
6. R. Villarreal, P.L. Varghese, *Appl. Opt.* **44**, 6786 (2005)
7. F. Wang, K.F. Cen, N. Li, J.B. Jeffries, Q.X. Huang, J.H. Yan, Y. Chi, *Meas. Sci. Technol.* **21**, 10 (2010)
8. P. Wright, N. Terzija, J.L. Davidson, S. Garcia-Castillo, C. Garcia-Stewart, S. Pegrum, S. Colbourne, P. Turner, S.D. Crossley, T. Litt, S. Murray, K.B. Ozanyan, H. McCann, *Chem. Eng. J.* **158**, 2 (2010)
9. F. Stritzke, O. Diemel, S. Wagner, *Appl. Phys. B* **119**, 143 (2015)
10. Z. Wang, S.T. Sanders, M.A. Robinson, *Appl. Phys. B* **122**, 1 (2016)
11. G. Schulze, A. Jirasek, M.M.L. Yu, A. Lim, R.F.B. Turner, M.W. Blades, *Appl. Spectrosc.* **59**(545), 15 (2005)
12. W.Y. Peng, R. Sur, C.L. Strand, R.M. Spearrin, J.B. Jeffries, R.K. Hanson, *Appl. Phys. B* **122**, 1 (2016)
13. E. Schleicher, M.J. da Silva, S. Thiele, A. Li, E. Wollrab, U. Hampel, *Meas. Sci. Technol.* **19**, 094006 (2008)
14. X. Li, L. Ma, *Opt. Express* **22**, 4768 (2014)